Available online at BCREC website: https://bcrec.id

Bulletin of Chemical Reaction Engineering & Catalysis, 18 (2) 2023, 210-221

Research Article

Polyoxometalate Intercalated M^{2+}/Al (M^{2+}=Ni, Mg) Layered Double Hydroxide for Degradation of Methylene Blue

Yulizah Hanifah[1], Risfidian Mohadi[1,2], M. Mardiyanto[3], Nur Ahmad[1,2], S. Suheryanto[1,2], Aldes Lesbani[1,2,*]

[1]Graduate School of Mathematics and Natural Sciences, Faculty of Mathematics and Natural Sciences, Universitas Sriwijaya, Jl. Palembang Prabumulih Km. 32 OganIlir 30662, Indonesia.
[2]Research Center of Inorganic Materials and Coordination Complexes, Faculty of Mathematics and Natural Sciences, Universitas Sriwijaya, Jl. Palembang Prabumulih Km. 32 OganIlir 30662, Indonesia.
[3]Department of Pharmacy, Faculty of Mathematics and Natural Sciences, Universitas Sriwijaya, Jl. Palembang Prabumulih Km. 32 OganIlir 30662, Indonesia.

Received: 28th March 2023; Revised: 14th May 2023; Accepted: 15th May 2023
Available online: 18th May 2023; Published regularly: July 2023

Abstract

The synthesis and characterization of M^{2+}/Al (M^{2+}=Ni, Mg) layered double hydroxide (LDH) and intercalated polyoxometalate is presented. We have reported the growth of polyoxometalate on Ni/Mg layered double hydroxide for degradation methylene blue (MB). By considering variables such as pH of dye solution, dye concentration, and time as degradation variables, the efficiency of organic dye degradation and degradation parameters of M^{2+}/Al (M^{2+} = Ni, Mg) LDH and both composite LDH-polyoxometalate has been identified. X-Ray Diffraction (XRD), Fourier Transform Infra Red (FTIR), Scanning Electron Microscope (SEM), and Ultra Violet Diffuse Reflectance Spectroscopy (UV-DRS) spectroscopy confirmed the layered double hydroxide structure. XRD and FTIR analysis confirmed the single-phase of the as-made and polyoxometalate intercalated LDH. SEM images show the formation of aggregates of small various sizes. The material's photodegradation was assessed through methylene blue (MB) degradation process. The result showed that NiAl-Si has a good degradation capacity for MB as compared to NiAl-Pw, MgAl-Si, and MgAl-PW. The result shows that LDH composite presents stability and has good photocatalytic activities toward the reduction of methylene blue. The FTIR measurement confirming the LDH composite structure reveals the materials used in the fifth regeneration. The activity of MB photodegradation pristine were NiAl (45%), MgAl (43%), NiAl-Pw (78%), NiAl-Si (85%), MgAl-Pw (58%), and MgAl-Si (75%), respectively. The LDH-polyoxometalate composite material's capacity to successfully photodegrade, as measured by the percentage of degradation, revealed an increase in photodegradation catalysis and the ability of the LDH to regenerate.

Keywords: LDH; LDH-polyoxometalate; photocatalyst; methylene blue

How to Cite: Y. Hanifah, R. Mohadi, M. Mardiyanto, N. Ahmad, S. Suheryanto, A. Lesbani (2023). Polyoxometalate Intercalated M^{2+}/Al (M^{2+}=Ni, Mg) Layered Double Hydroxide for Degradation of Methylene Blue. *Bulletin of Chemical Reaction Engineering & Catalysis*, 18 (2), 210-221 (doi: 10.9767/bcrec.17789)

Permalink/DOI: https://doi.org/10.9767/bcrec.17789

1. Introduction

According to its chemical makeup, the methylene blue dye (3,7-bis(dimethylamino)-phenothiazine-5-iumchloride;MB) is an azo dye, and depending on how it is used, it is either a cationic dye or a basic dye [1]. Figure 1 shows the structure of methylene blue. Water containing organic pollutants and an organic dye used in industrial applications are the principal contaminants, specifically in aquaculture due to its uses as an antibacterial agent. It is also used as

* Corresponding Author.
Email: aldeslesbani@pps.unsri.ac.id (A. Lesbani)

a dyeing agent for wool, paper, leather, etc. However, it also has a wide range of negative side effects, particularly for mammals, including mutagenesis, carcinogenicity, and deformity [2].

Dye and organic molecules cause severe consequences for the ecosystem. The two main classes of the organic components are autochromes and chromophores [3]. Organic dyes are frequently found as harmful pollutants in leather, paper. Biowaste and industrial activated carbon products, plastics, textiles, food, and the cosmetics industry [4]. The dye used in the textile industry alters the lakes, oceans, and rivers to the point where they resemble watercolors, causing biological and chemical changes that could harm the fish. Significant health issues for humans result from harming living things and taking lives. To remove the organic pigment from water, conventional techniques such filtration, coagulation, biological processes, and precipitation have been used. One of the drawbacks of the adsorption, coagulation, and precipitation method is that the dye waste still has a fixed structure in the process so its toxicity is still high. Recently, treatment was used to degrade dyes from wastewater via photocatalysis [5]. Photocatalysis is a green treatment technology, due of its low cost, good performance, and great efficiency, one of the most promising technologies, according to experts [6,7]. The photodegradation process is still regarded as being most beneficial to remove dyes from water are thus easily and effectively eliminated [8], porous carbon, and other materials have all been used with the photocatalyst to remove colors from aqueous solutions [9,10]. According to Yang *et al.* [11], implementing ZnAl-LDH successfully degrades methylene blue. Tabatabaeian *et al.* [12] confirmed that BNC-Cls modified with NiAl-LDH successfully removed methylene blue dye reached to 84%. Guo *et al.* [13] successfully degraded methylene blue with TiO_2.

Layered double hydroxide (LDH), which has brucite-like layers with positively charged multimetal cations and interlayer compensating anions, has been employed for the removal of

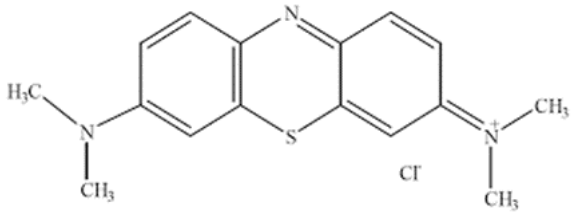

Figure 1. The structures of the methylene blue (MB).

pollutants. LDH has the general formula $M_{1-x}^{2+}M_x^{3+}(OH)_2]^{x+}(A^n)_{x/n}\cdot mH_2O$ where M^{2+} and M^{3+} are trivalent metals (Al, Fe, Cr) and divalent metal cations (Ca, Mg, Co, Fe, Cu, Ni, Mn). A is the anion that is between the layers of valence n (Cl^-, NO^{3-}, ClO^{4-}, CO^{3-}, SO^{4-} and so on), and the value of x is equal to the molar ratio of $M^{3+}/(M^{2+} + M^{3+})$, where the value is between 0.20 and 0.33 [14]. Recent LDH research has focused on energy storage, heavy metal ions, adsorbents, and other techniques to r move pollutants from wastewater (both organic and inorganic) [15,16]. Due to its shape, a single LDH is not thought to be an effective catalyst [17]. The structural properties of LDHs allow for the significant improvement of catalytic performance by using a variety of control synthesis methods, such as intercalated and immobilized, to modify the active centers and morphology (such as flaws, crystal faces, and electrical states) [18–20]. However, in its utilization, the hydroxy double layered is still out used effectively as a catalyst because it has a small interlayer spacing and low density in the activity side of its surface area, so it needs to be modified so that the surface area increases and the activity increase [21].

As a result, the use of LDH as a photocatalyst to decompose organic contaminants, according to a recent study has been established with a variety of components. LDH composite has greater performance than LDH pristine, according to Yuliasari *et al.* [22] which claimed that metal oxide affected LDH (ZnAl and MgAl) for decomposing MG [23]. Bi_2O_3 successfully degraded methyl orange [24]. Bi_2O_3 synthesis with $H_2C_2O_4$ resulted higher on degrading methyl orange compared with Bi_2O_3 synthesis using Na_2CO_3 [25]. NiCo-LDH composited with transition metal phosphide (Ni_2P) was effectively produced and applied to degraded tetracycline to increase photodegradation process [20]. According to Guo *et al.* [13], they are composite synthesized, exhibit more severe degradation, and exhibit composite CoAl-primary CeO_2's photocatalytic activity. We successfully synthesized [26], respectively. The cation-anion exchange capacity, high adjustable band gap, and adsorption capacity of LDH materials enable them to create spatially separated redox reaction sites. Ni and Mg LDH are capable on photocatalysts on degradation dye. NiAl-LDH [27] and MgAl-LDH [28] modified with polyoxometalate successfully degraded malachite green. La-doped NiFe-layered double hydroxides containing polyoxometalate interlayer were synthesized and applied as catalyst for the removal of peroxymonosulfate [29]. Fur-

thermore, LDHs feature a wide range of morphological benefits and adaptable compositions, including an interlayered arrangement of mortal ions, varied chemical compositions, and the capacity to interchange anions on layers [30] as well as LDH materials, which have a highly adjustable adsorption capacity, band gap, and the ability to create spatially isolated redox reaction sites [31].

In the present study, Mg and Ni LDH that was mainly composited of two different polyoxometalates (POM) type Keggin $K_3[\alpha\text{-}PW_{12}O_{40}]$ and $K_4[\alpha\text{-}SiW_{12}O_{40}]$ were created using the co-precipitation method, and the effects of pH, contact duration, catalyst loading, and material regeneration on their photocatalytic performances were examined. Because POM anions have a large negative charge and can improve the performance of cationic dye, which can perform photodegradation methylene blue (MB) dye, we choose POM as intercalate to composite with Mg and Ni LDH. Both materials modified were un yet used for the photodegradation of methylene blue. The substance is used as a photocatalyst to decompose MB dye. FTIR, XRD, SEM, and UV-DRS were all utilized to describe the produced material. Also, this study used the application as a photocatalyst to carry out the process of photodegradation, particularly pH affects, contact duration time, catalyst loading, and reusable of material.

2. Materials and Methods

2.1 Chemicals

Aluminum nitrate ($Al(NO_3)_3$), magnesium nitrate ($Mg(NO_3)_2$), sodium phosphate (Na_3PO_4), nickel nitrate ($Ni(NO_3).6H_2O$), sodium carbonate (Na_2CO_3), sodium tungstate (Na_2WO_4), sodium hydroxide (NaOH), and concentrated hydrogen chloride (HCl) were used without any furtherer purification and were purchased from Sigma Aldrich and Merck. One of the synthetic dyes with the formula methylene blue (MB) is $C_{16}H_{18}CIN_3S$ and maximum absorbency at λ_{max} 665 nm.

2.2 Characterization

The materials LDH pristine and LDH composite catalyst were characterized with Shimadzu FTIR ALPHA Bruker (Platinum-ATR) is used. By using Rigaku XRD Miniflex-6000 diffractometer, Cu-Kα as the radiation source, 30 kV voltage, 10 mA electricity, and 2θ ranging from 10° to 90°, XRD was analyzed. The UV-Vis Biobase BK-UV 1800 PC spectrophotometer was used to measure the degradation of MB dye between 660-668 nm. SEM FEI Quanta 650 was used to carry out SEM analysis. The UV-Vis JASCO V-760 was used to do a band gap analysis utilizing a UV-Vis diffuse reflectance spectrometer.

2.3 Synthesis of M^{2+}/Al (M^{2+}=Ni, Mg)

Aluminum nitrate 0.25 M and magnesium nitrate 0.75 M were dissolved in water (100 mL) and stirred for two hours. Through the use of a modified co-precipitation process, the catalyst was created. Sodium hydroxide was added to the mixture to bring the pH below to 10. To create MgAl-LDH, this combination was agitated for six hours at 85 °C. NiAl-LDH was created using the same method as MgAl-LDH; mixing nickel nitrate 0.75 M and aluminum nitrate 0.25 M dissolved in water 200 mL and stirring for two hours. To achieve a pH of 8, 2 M sodium hydroxide was then agitated for 4 hours at 343 K to produce NiAl-LDH.

2.4 Preparation of Composite

Solution A is 2 g of polyoxometalate compound and 50 mL of distilled water were used to create the composite. Solution B is 2 g of material catalyst (pristine and composite LDH) in 25 mL of sodium hydroxide 1 M. In order to create the composite LDH, the suspension was mixed right away with N_2 gas for 24 hours. The product of composite LDH will be characterized using XRD analysis, FTIR spectrophotometer, SEM analysis, and UV-DRS to analyze the composite LDH product. $K_3[\alpha\text{-}PW_{12}O_{40}].nH_2O$ and $K_4[\alpha\text{-}SiW_{12}O_{40}].nH_2O$ polyoxometalate, according to previously publish literature, was created [32].

2.5 Photocatalytic Study

The composite was used dissolve solution of the methylene blue. To achieve a desorption equilibrium, methylene blue was first immersed in the darkened and magnetically agitated for 30 min with an ideal catalyst weight of 20 mg/L. Then, 20 mg/L of methylene blue were used in the photocatalytic test that was conducted at regular intervals. For catalyst loading at 75, 100, 250, 500, and 750 mg respectively, and for degradation contact time at 10, 20, 30, 40, 50, 60, 70, 80, 90, 100, 110, and 120 minutes, optimization degradation incorporates variations in pH ranges (3, 5, 7, 9, and 11). This degradation process is carried out using UV light W (4 × 20 watt) on wavelength 665 nm. The following equation formula is used to define the percentage of degradation:

Degradation rate in percentage (%) = (C_o – C_t)/Together x 100, where C_o is the dye concentration at the beginning of the degradation process and C_t is the dye concentration after the process has finished [33].

2.6 Regeneration Experiment

The initial reaction's suspension created a solid powder that was then centrifuged and used to test the photocatalyst's repeatability of the photocatalyst. The solution and the suspension were separated by a precipitate. The precipitate powder was then dried for 24 h at 70 °C. The following photocatalytic reaction was carried out on the solid powder. The confirmation of the reproducibility of both the LDH pristine and LDH composite photocatalyst, the above method was carried out a fifth time.

3. Results and Discussion

3.1 LDH Pristine and Composite

On Figure 2, XRD analysis of LDH pristine and LDH composites were made. The X-Ray diffraction pattern of pure polyoxometalate compounds which are $K_4[\alpha\text{-}SiW_{12}O_{40}]$, $K_3[\alpha\text{-}PW_{12}O_{40}]$, LDH pristine NiAl-LDH, MgAl-LDH, and LDH composite are shown in Figure 2. The LDH crystal plane is shown by LDH pristine diffraction peaks at 11.58°, 23.18°, 35.01°, 39.41°, 46.70°, 60.94° and 62.26° which correspond to the (003), (006), (012), (015), (018), (110) and (113) correspondingly, indicate the LDH crystal plane (JCPNDF No. 22-0452) [34]. The diffraction of polyoxometalate compound $K_4[\alpha\text{-}SiW_{12}O_{40}]$, $K_3[\alpha\text{-}PW_{12}O_{40}]$ was shown at 2θ angles of 8-20°, 25-30° [35]. Due to the utilization of composite LDH and polyoxometalate on MgAl-LDH. According to Figure 2, each polyoxometalate peak in MgAl-$PW_{12}O_{40}$ that was at angles 7.73°, 28.6°, 35.6° which correspond to the (003), (006) and (009) is still visible. $K_4[\alpha\text{-}SiW_{12}O_{40}]$ is present in LDH, however, as shown by the 2 angles of 8.61°, 24.27°, 34.96° and 66.34°. The synthesis of the composites was successful. The successfully intercalated of NiAl composite material by showing angles at 10.76°, 26.59°, 30.8° and 63.11°. Each material was shown the LDH pristine by peak 003 indicating that the material contains carbonate

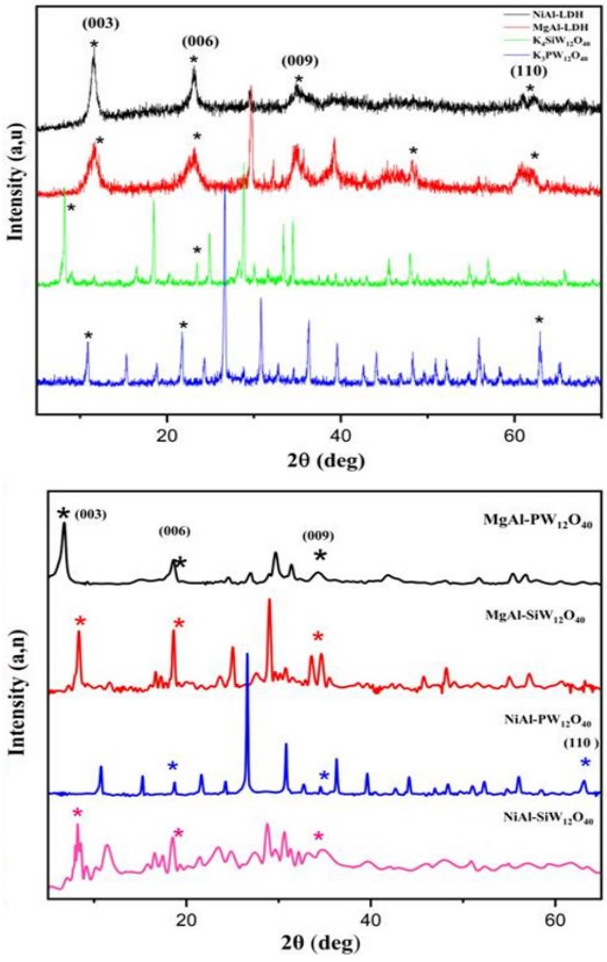

Figure 2. Diffractogram of catalyst.

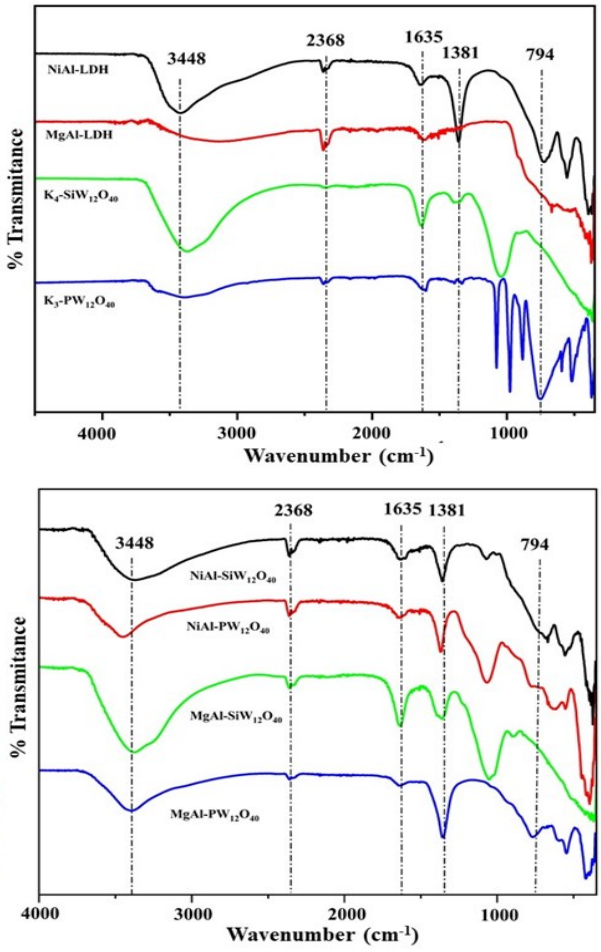

Figure 3. FTIR analysis of catalyst.

and nitrate anions. Nevertheless the typical of polyoxometalate compound in this study showed diffraction at angles 8.26°, 11.34°, 29° and 35.1°.

Figure 3 shows the infrared spectrum of LDH pristine and LDH composite. Spectrum of polyoxometalate compound was measured. The alfa-Keggin SiW_{12} exhibits four distinctive asymmetric vibration bands that correspond to 927, 973, 882, and 813 cm^{-1} in the range 780-980 cm^{-1} indicated of W−O [36]. By using FTIR analysis, the surface groups of LDH were identified. The composites synthesis was successful. The finding of FTIR characterization of LDH pristine and LDH composite is displayed in Figure 2. The FTIR spectrum band between 3420–3500 cm^{-1} was shown brucite-like layers and interlayer water molecules. This band was shown for all material pristine and material composite. The absorption of medium intensity (H_2O) from interlayer water is also close to 1630 cm^{-1}. The 1381 cm^{-1} band represents the CO_3 vibrations [37]. In the bands of 983-870 cm^{-1} and 804.84 cm^{-1}, respectively, represent the W−O and W−O−W bands [35]. These bands can still be seen in their typical LDH-polyoxometalate catalyst state, as seen in Figure 3.

SEM analysis was used to analyse the morphology of the subsequently synthesized MgAl-LDH, as seen in Figure 4. The MgAl-LDH samples showed morphology, demonstrating the validity of the LDH microsphere to the layered framework. LDH composite and LDH pristine

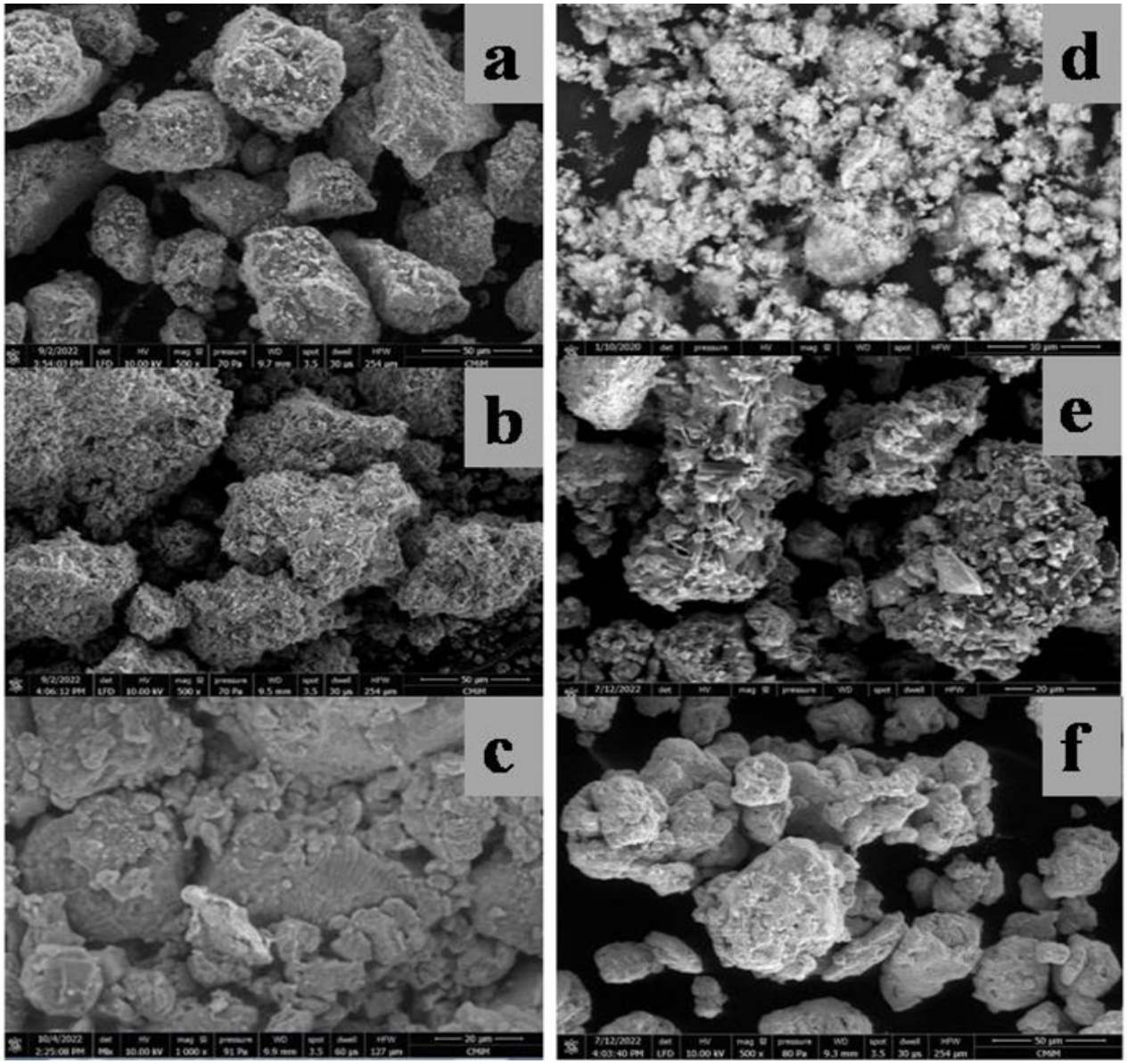

Figure 4. (a) MgAl-LDH, (b) MgAl-$[SiW_{12}O_{40}].nH_2O$, (c) MgAl-$[PW_{12}O_{40}].nH_2O$, (d) NiAl-LDH, (e) NiAl-$[PW_{12}O_{40}].nH_2O$, and (f) NiAl-$[PW_{12}O_{40}].nH_2O$ SEM.

have different heterostructures. The morphology which appears to be created by the assembly the two-layered materials is proof that LDH intercalated heterostructures are present. When [$SiW_{12}O_{40}$], the aggregate appeared on the surface material, according to the morphological structure. It is feasible to understand that platelet-shaped microcrystals exist. If the LDH composite is compared to the LDH pristine, was polypore which meant introducing polyoxometalate added to the blending solution has the potential to bond to the composite's surface. The percentage of Ni, Al, W, P, Si, K, Cl, C, O, and Na atoms are shown in Table 1 of the EDX research. After being composited into MgAl-[$SiW_{12}O_{40}$] and MgAl-[$PW_{12}O_{40}$].

3.2 Impact of Optimization Parameters on Methylene Blue Degradation

The stability of the LDH structure may be impacted by the impact of polyoxometalate on MB degradation pH in MgAl-[$SiW_{12}O_{40}$] and MgAl-[$PW_{12}O_{40}$]. The capacity to generate positively charged electron holes can be improved by increasing the number of anionic species, especially in media pH levels below 7, which are capable of producing OH• radicals that can degrade dyes and also cause the polyoxometalate to photodegrade into ions. The decomposition of polyoxometalate into their ions is also possible when the pH is low. There is a photocatalytic reaction of LDH-POM, a UV-irradiated catalyst LDH-POM produces a hole (h_{vb}^+). The hole in the valence reacts with hydroxyl (OH^-) anion that form a hydroxyl radical (•OH) which can degrade methylene blue and become simply intermediate [38]. The following stage of the process uses LDH-POM to demonstrate the photocatalysis mechanism (Figure 5):

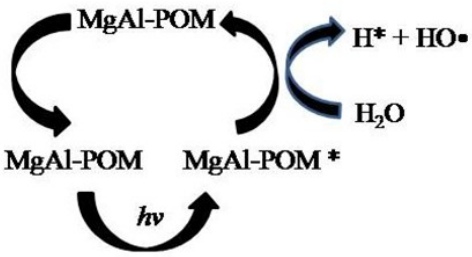

Figure 5. MgAl-POM-based process mechanism for photocatalysis.

$$\text{LDH-[POM]} + h\upsilon \rightarrow \text{LDH-[POM]} (e_{cb}^- + h_{vb}^+)$$
$$h_{vb}^+ + H_2O \rightarrow H^+ + OH^-$$
$$h_{vb}^+ + OH^- \rightarrow OH$$
$$\text{•OH + Methylene Blue} \rightarrow CO_2 + H_2O + \text{simpler compounds}$$

This causes in this study MgAl-LDH and NiAl-LDH were obtained at pH 11 and pH 7 while, pH 11 for $K_3[\alpha\text{-}PW_{12}O_{40}]$ and $K_4[\alpha\text{-}SiW_{12}O_{40}]$, while for composite material, such as MgAl-[$PW_{12}O_{40}$], is optimum at pH 1, MgAl-[$SiW_{12}O_{40}$] is optimum at pH 5, NiAl-[$PW_{12}O_{40}$] and NiAl-[$PW_{12}O_{40}$] at pH 11, respectively. Figure 6 demonstrates the impact of pH on the degradation of methylene blue by both pristine and composite LDH catalysts.

In this study, the impact of catalyst weight on the degradation process was also investigated by applying it for 100 min at the ideal pH. Figure 7 shows the actual effect of different loading catalysts on the degrading MB by both LDH pristine and LDH composite, where it is evident that the degradation percentages of the two materials are equivalent. The impact of MB degradation contact time variations by both material catalyst LDH composite and LDH pristine is demonstrated in Figure 7. After 100 min of the treatment, the value of C/Co increased, and as time went on, more MB was

Table 1. Catalysts EDX.

Element	MgAl-LDH (%wt)	MgAl-Pw (%wt)	MgAl-Si (%wt)	NiAl-LDH (%wt)	NiAl-Pw (%wt)	NiAl-Si (%wt)
Ni	-	-	-	88.3	4.9	3.7
Mg	8.14	6.32	2.51	-	-	-
Al	5.20	6.85	1.62	1.3	1.7	1.0
W	-	2.15	32.54	-	44.7	19.5
P	-	-	7.82	-	0.7	-
Si	-	-	-	-	-	0.9
K	-	-	3.53	-	2.7	4.9
Cl	-	-	9.17	-	-	7.9
C	13.57	7.98	8.20	-	14.5	24.2
O	51.39	45.85	28.78	9.1	25.6	27.8
Na	2.58	4.1	5.83		4.9	9.6
N	9.12	-	-	1.4	-	-

degraded. The percent MB degradation for MgAl-LDH, NiAl-LDH, MgAl-[$PW_{12}O_{40}$], MgAl-[$SiW_{12}O_{40}$], NiAl-[$PW_{12}O_{40}$], NiAl-[$SiW_{12}O_{40}$] were 43.14%, 45.53%, 58.73%, 75.94%, and 85.86%, respectively. The percent degradation for $K_3[\alpha\text{-}PW_{12}O_{40}]$ and $K_4[\alpha\text{-}SiW_{12}O_{40}]$ were 73.14% and 78.79%, respectively. According to the percentage decomposition results, the catalyst of LDH composite appears to have a greater capacity to degrade MB than LDH pristine.

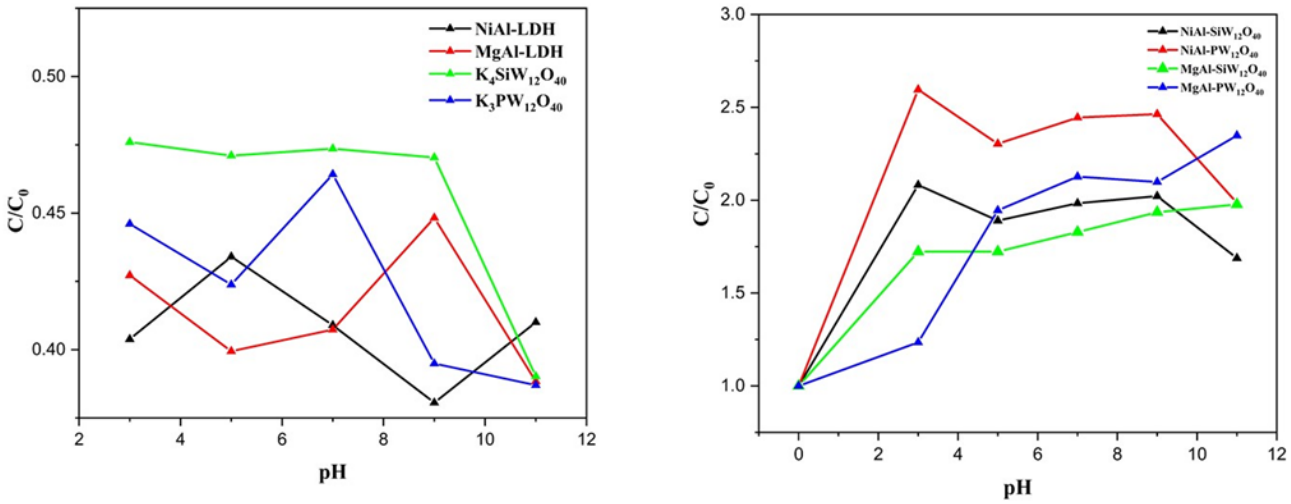

Figure 6. Impact of pH on catalyst mediated MB degradation.

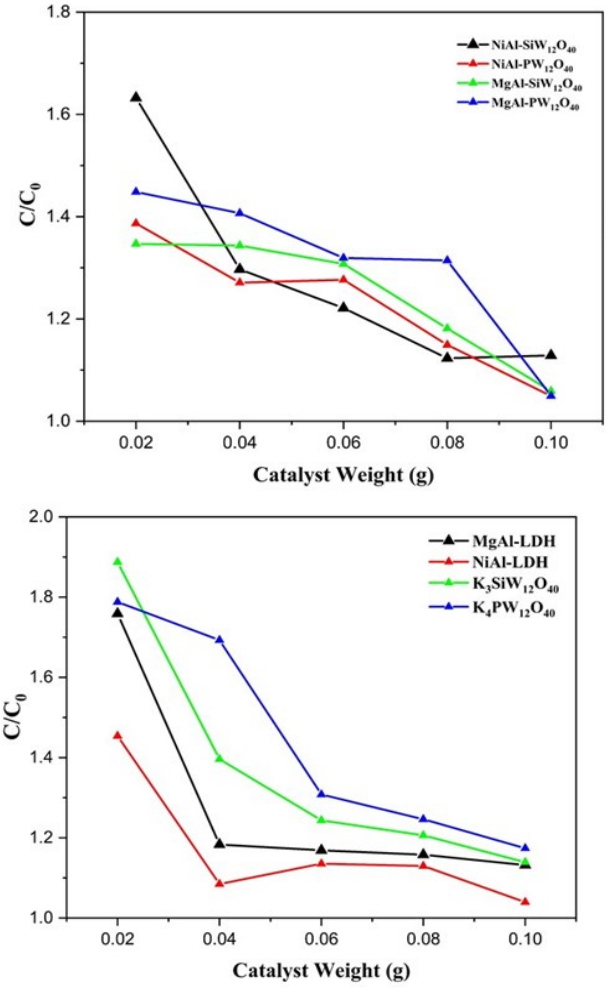

Figure 7. Effect of catalyst weight on MB degradation.

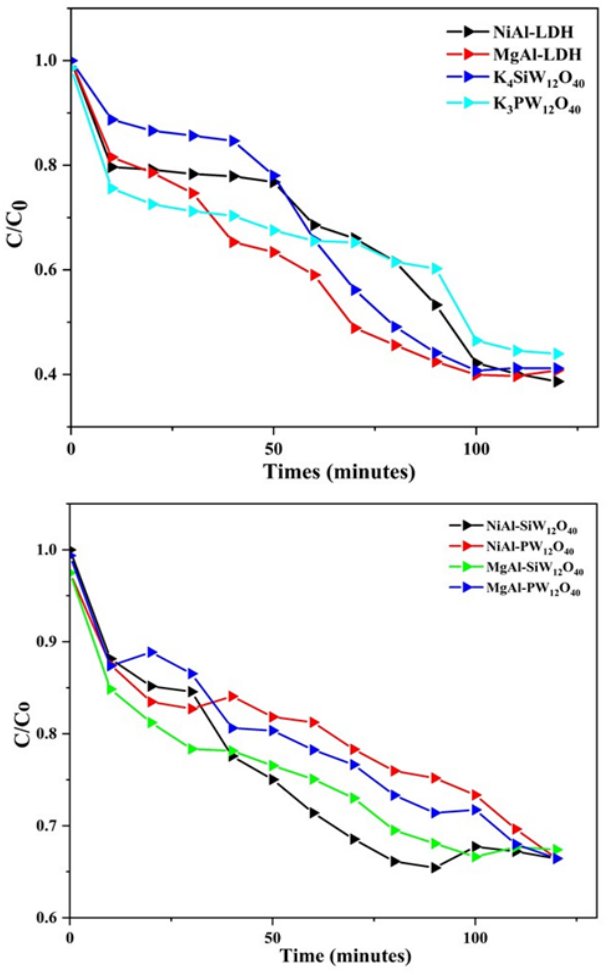

Figure 8. Effect of time on catalytic degradation of MB.

Figure 8 shows for all materials increased the %degradation process by increased contact time effect.

3.3 Regeneration of Catalyst

Indicating that the catalyst's use is anticipated to be effective so that it can be used frequently to degrade organic pollutants, its capacity is determined by the decline in the percentage of degradation after several cycles of repeated usage. After being used again as a photocatalyst, the deteriorating ability is shown to decreased in Figure 9. After five cycles, the degradation rate using the MgAl-LDH and NiAl-LDH catalyst was reduced by 46.1% and 55.3%. After 5 cycles of usage, MgAl-[$PW_{12}O_{40}$], MgAl-[$SiW_{12}O_{40}$], NiAl-[$PW_{12}O_{40}$] and NiAl-[$SiW_{12}O_{40}$] reduced LDH composite degradation by 63.4%, 70.4%, 72%, and 83%, respectively. The apparent rate value and percentage of deterioration matched the reusability of both pristine and composite LDH. The %degradation and apparent rate value matched the reusability of all materials. Table 2 shows the value of %degradation methylene blue with different material. It is evident from the reusability data that the LDH-[$SiW_{12}O_{40}$] exceeded the LDH-[$PW_{12}O_{40}$].

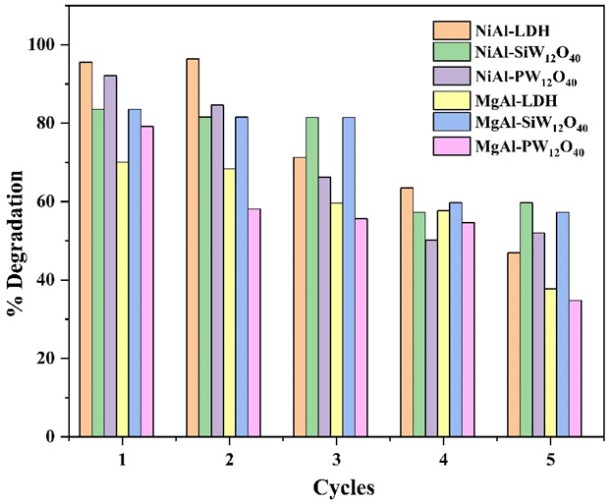

Figure 9. Catalyst regeneration in fifth cycle.

Figure 10 shows FTIR spectra of all materials MgAl-LDH, NiAl-LDH, $K_4[\alpha\text{-}SiW_{12}O_{40}]$, $K_3[\alpha\text{-}PW_{12}O_{40}].nH_2O$, MgAl-[$SiW_{12}O_{40}$], MgAl-[$PW_{12}O_{40}$], NiAl-[$SiW_{12}O_{40}$], and NiAl-[$PW_{12}O_{40}$]. The interpretation of stretching and bending vibration of FTIR spectra revealed the

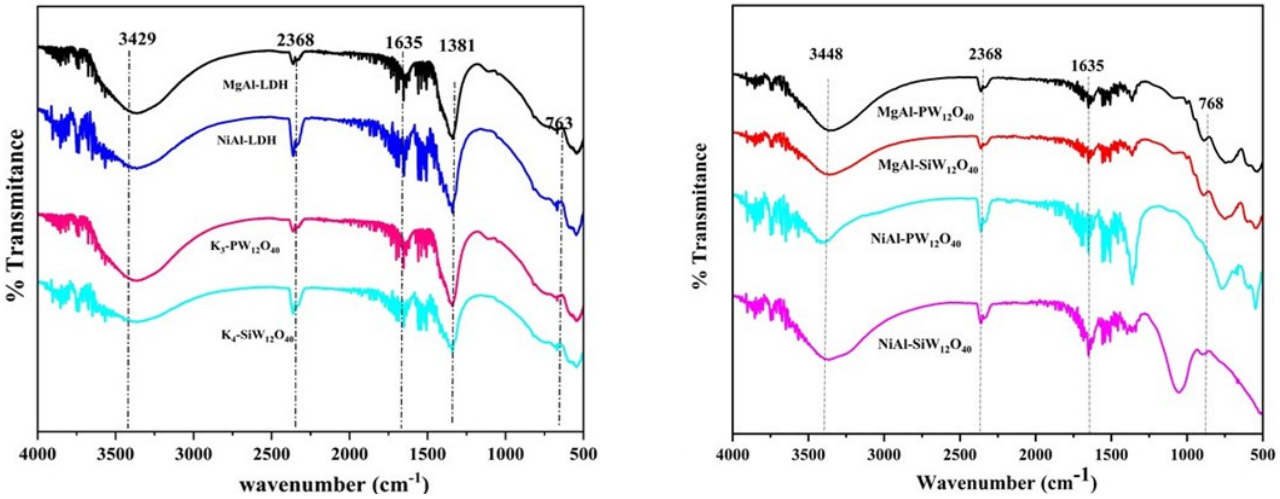

Figure 10. FTIR spectrum following a fifth cycle regeneration.

Table 2. The value of %degradation methylene blue.

Catalyst	%degradation methylene blue	Ref.
Mn_2Cr-LDH	81	[39]
Mn-ZnO	83	[40]
Zn/Al	75	[41]
BNC-CLs	84	[42]
MnMgFe-LDH	80	[43]
MgAl-[$PW_{12}O_{40}$]	58	In this study
MgAl-[$SiW_{12}O_{40}$]	75	In this study
NiAl-[$PW_{12}O_{40}$]	78	In this study
NiAl-[$SiW_{12}O_{40}$]	85	In this study

good formation of MgAl-LDH, NiAl-LDH, $K_4[\alpha\text{-}SiW_{12}O_{40}]$, $K_3[\alpha\text{-}PW_{12}O_{40}]$, and MgAl-$[SiW_{12}O_{40}]$, MgAl-$[PW_{12}O_{40}]$, NiAl-$[SiW_{12}O_{40}]$, and NiAl-$[PW_{12}O_{40}]$. LDH composite that needed to degrade MB was characterized using an FTIR spectrum to show the effect upon regeneration. The unlimited range a bands with wavelengths between 3420–3500 cm^{-1} and around 1630-1583.6 cm^{-1} included the stretching vibration of the hydroxyl groups coupled with the stretching vibration of interlayer water molecules. The intercalated NO_3^- bending vibration is represented by the peak at 1359 cm^{-1} [44]. The W−O and W−O−W bands, which are typical of polyoxometalate, are in the 985.4 cm^{-1} and 856.3 cm^{-1} ranges, respectively. The band on MgAl-$[PW_{12}O_{40}]$ are also demonstrated to be 795.4 [45]. Ta from the IR spectra $[PW_{12}O_{40}]$ are still stored in the LDH. Figure 10 demonstrates that for the catalyst that has degraded MB, where these band are still visible.

4. Conclusion

Successful preparation and usage of the LDH pristine and LDH composite for photodegradation MB. Based on the characterization findings, the materials that were synthesized in the best way had layer structures that were well-oriented. The capacity to photodegrade cationic dyes MB was improved by modifying LDH material, which forms composites with two polyoxometalates $[\alpha\text{-}PW_{12}O_{40}]$ and $[\alpha\text{-}SiW_{12}O_{40}]$. In comparison to MgAl-LDH, composite MgAl-$[PW_{12}O_{40}]$ and MgAl-$[SiW_{12}O_{40}]$ composites both enhanced MB degradation regeneration performance. Materials that have degraded MB were characterized by FTIR after the fifth cycle of regeneration, and the results showed that all materials LDH pristine and LDH composite both still had their original LDH and polyoxometalate structures. The investigation's finding on pH, catalyst loading, and ideal contact time revealed percentages of degradation and reusability.

Acknowledgment

The authors thank to Research Center of Inorganic Materials and Complexes FMIPA Universitas Sriwijaya for valuable discussion, apparatus, and chemical analysis.

CRediT Author Statement

Author Contribution: Yulizah Hanifah: Experiment, Methodology, Investigation, Resorces, data Curation, Writing, Review and Editing, Supervision; Risfidian Mohadi: Review, Formal Analysis and Data Curation; M. Mardiyanto: Review and Data Curation; Nur Ahmad: Review and Data Curation; S. Suheryanto: Review and Data Curation; Aldes Lesbani : Review, Formal Analysis, Editing and Data Curation. All authors have read and agreed to the published version of the manuscript.

References

[1] Basaleh, A.A., Al-Malack, M.H., Saleh, T.A. (2019). Methylene Blue removal using polyamide-vermiculite nanocomposites: Kinetics, equilibrium and thermodynamic study. *Journal of Environmental Chemical Engineering*, 7(3), 103107. DOI: 10.1016/j.jece.2019.103107.

[2] Salamat, S., Hadavifar, M., Rezaei, H. (2019). Preparation of nanochitosan-STP from shrimp shell and its application in removing of malachite green from aqueous solutions. *Journal of Environmental Chemical Engineering*, 7(5), 103328. DOI: 10.1016/j.jece.2019.103328.

[3] Zhou, L., Xu, K., Cheng, X., Xu, Y., Jia, Q. (2017). Study on optimizing production scheduling for water-saving in textile dyeing industry. *Journal of Cleaner Production*, 141, 721–727. DOI: 10.1016/j.jclepro.2016.09.047.

[4] Xu, M., Bi, B., Xu, B., Sun, Z., Xu, L. (2018). Polyoxometalate-intercalated ZnAlFe-layered double hydroxides for adsorbing removal and photocatalytic degradation of cationic dye. *Applied Clay Science*, 157, 86–91. DOI: 10.1016/j.clay.2018.02.023.

[5] Zhang, T.T., Hu, Y.Y., Zhang, X., Cui, X.B. (2020). New compounds of polyoxometalates and cadmium mixed-organic-ligand complexes. *Journal of Solid State Chemistry*, 283, 121168. DOI: 10.1016/j.jssc.2019.121168.

[6] Shi, Y., Huang, J., Zeng, G., Cheng, W., Hu, J. (2019). Photocatalytic membrane in water purification: is it stepping closer to be driven by visible light?. *Journal of Membrane Science*, 584, 364–392. DOI: 10.1016/j.memsci.2019.04.078.

[7] Lu, K., Li, Q., Xi, X., Zhou, T., Zhao, X. (2020). Metal-Free Difluoromethylselenolation of Arylamines under Visible-Light Photocatalysis. *Journal of Organic Chemistry*, 85(2), 1224–1231. DOI: 10.1021/acs.joc.9b02535.

[8] Khan, A.U., Khan, A.U., Li, B., Mahnashi, M.H., Alyami, B.A., Alqahtani, Y.S., Tahir, K., Khan, S., Nazir, S. (2020). A facile fabrication of silver/copper oxide nanocomposite: An innovative entry in photocatalytic and biomedical materials. *Photodiagnosis and Photodynamic Therapy*, 31, 101814. DOI: 10.1016/j.pdpdt.2020.101814.

[9] Zhang, S., Yan, Y., Wang, W., Gu, X., Li, H., Li, J., Sun, J. (2018). Intercalation of phosphotungstic acid into layered double hydroxides by reconstruction method and its application in intumescent flame retardant poly (lactic acid) composites. *Polymer Degradation and Stability*, 147, 142–150. DOI: 10.1016/j.polymdegradstab.2017.12.004.

[10] Ding, N., Zhang, L., Zhang, H., Shi, J., Wu, H., Luo, Y., Li, D., Meng, Q. (2017). Microwave-assisted synthesis of $ZnIn_2S_4$/g-C_3N_4 heterojunction photocatalysts for efficient visible light photocatalytic hydrogen evolution. *Catalysis Communications*, 100, 173–177. DOI: 10.1016/j.catcom.2017.06.050.

[11] Yang, J., Jing, R., Wang, P., Liang, D.R., Huang, H., Xia, C., Zhang, Q., Liu, A., Meng, Z., Liu, Y. (2021). Black phosphorus nanosheets and ZnAl-LDH nanocomposite as environmental-friendly photocatalysts for the degradation of Methylene blue under visible light irradiation. *Applied Clay Science*, 200, 105902. DOI: 10.1016/j.clay.2020.105902.

[12] Tabatabaeian, R., Dinari, M., Aliabadi, H.M. (2021). Cross-linked bionanocomposites of hydrolyzed guar gum/magnetic layered double hydroxide as an effective sorbent for methylene blue removal. *Carbohydrate Polymers*, 257, 117628. DOI: 10.1016/j.carbpol.2021.117628.

[13] Guo, X., Fan, Z., Wang, Y., Jin, Z. (2021). CeO_2 nanoparticles dispersed on CoAl-LDH hexagonal nanosheets as 0D/2D binary composite for enhanced photocatalytic hydrogen evolution. *Surfaces and Interfaces*, 24, 101105. DOI: 10.1016/j.surfin.2021.101105.

[14] Malherbe, F., Besse, J.P. (2000). Investigating the effects of guest-host interactions on the properties of anion-exchanged Mg-Al hydrotalcites. *Journal of Solid State Chemistry*, 155(2), 332–341. DOI: 10.1006/jssc.2000.8922.

[15] Yoshida, M., Koilraj, P., Qiu, X., Hirajima, T., Sasaki, K. (2015). Sorption of arsenate on MgAl and MgFe layered double hydroxides derived from calcined dolomite. *Journal of Environmental Chemical Engineering*, 3(3), 1614–1621. DOI: 10.1016/j.jece.2015.05.016.

[16] Behbahani, E.S., Dashtian, K., Ghaedi, M. (2020). Fe/Co-chalcogenide-stabilized Fe_3O_4 nanoparticles supported MgAl-layered double hydroxide as a new magnetically separable sorbent for the simultaneous spectrophotometric determination of anionic dyes. *Microchemical Journal*, 152, 104431. DOI: 10.1016/j.microc.2019.104431.

[17] Kaul, P.K., Samson, A.J., Selvan, G.T., Enoch, I.V.M.V., Selvakumar, P.M. (2017). Synergistic effect of LDH in the presence of organophosphate on thermal and flammable properties of an epoxy nanocomposite. *Applied Clay Science*, 135, 234–243. DOI: 10.1016/j.clay.2016.09.031.

[18] Tonda, S., Jo, W.K. (2018). Plasmonic Ag nanoparticles decorated NiAl-layered double hydroxide/graphitic carbon nitride nanocomposites for efficient visible-light-driven photocatalytic removal of aqueous organic pollutants. *Catalysis Today*, 315, 213–222. DOI: 10.1016/j.cattod.2017.12.019.

[19] Wang, R., Su, S., Ren, X., Guo, W. (2021). Polyoxometalate intercalated La-doped NiFe-LDH for efficient removal of tetracycline via peroxymonosulfate activation. *Separation and Purification Technology*, 274, 119113. DOI: 10.1016/j.seppur.2021.119113.

[20] Sun, Y., Wang, X., Fu, Q., Pan, C. (2021). A novel hollow flower-like 0D/3D $Zn_{0.5}Cd_{0.5}S$/NiCoZn-LDH photocatalyst with n-n heterojunction for high hydrogen production. *Applied Surface Science*, 564, 150379. DOI: 10.1016/j.apsusc.2021.150379.

[21] Starukh, H., Levytska, S. (2019). The simultaneous anionic and cationic dyes removal with Zn–Al layered double hydroxides. *Applied Clay Science*, 180, 105183. DOI: 10.1016/j.clay.2019.105183.

[22] Yuliasari, N., Wijaya, A., Amri, Mohadi, R., Elfita, Lesbani, A. (2022). Application of M^{2+} (Magnesium, Zinc)/Alumina-Metal Oxide Composites as Photocatalysts for the Degradation of Cationic Dyes. *Ecological Engineering and Environmental Technology*, 23(4), 125–135. DOI: 10.12912/27197050/150374.

[23] Gholami, P., Khataee, A., Soltani, R.D.C., Dinpazhoh, L., Bhatnagar, A. (2020). Photocatalytic degradation of gemifloxacin antibiotic using Zn-Co-LDH@biochar nanocomposite. *Journal of Hazardous Materials*, 382, 121070. DOI: 10.1016/j.jhazmat.2019.121070.

[24] Astuti, Y., Arnelli, Pardoyo, Fauziyah, A., Nurhayati, S., Wulansari, A.D., Andianingrum, R., Widiyandari, H., Bhaduri, G.A. (2017). Studying impact of different precipitating agents on crystal structure, morphology, and photocatalytic activity of bismuth oxide. *Bulletin of Chemical Reaction Engineering & Catalysis*, 12(3), 478–484. DOI: 10.9767/bcrec.12.3.1144.478-484.

[25] Astuti, Y., Andianingrum, R., Arnelli, A., Haris, A., Darmawan, A. (2020). The Role of $H_2C_2O_4$ and Na_2CO_3 as Precipitating Agents on the Physichochemical Properties and Photocatalytic Activity of Bismuth Oxide. *Open Chemistry*, 18(1), 129–137. DOI: 10.1515/chem-2020-0013.

[26] Amini, M., Khaksar, M., Ellern, A., Keith Woo, L. (2018). A new nanocluster polyoxomolybdate $[Mo_{36}O_{110}(NO)_4(H_2O)_{14}]\cdot 52H_2O$: Synthesis, characterization and application in oxidative degradation of common organic dyes. *Chinese Journal of Chemical Engineering*, 26(2), 337–342. DOI: 10.1016/j.cjche.2017.03.031.

[27] Hanifah, Y., Mohadi, R., Mardiyanto, M., Lesbani, A. (2022). Photocatalytic Degradation of Malachite Green by NiAl-LDH Intercalated Polyoxometalate Compound. *Bulletin of Chemical Reaction Engineering & Catalysis*, 17(3), 627–637. DOI: 10.9767/bcrec.17.3.15418.627-637.

[28] Hanifah, Y., Mohadi, R., Mardiyanto, Lesbani, A. (2023). Polyoxometalate Intercalated MgAl-Layered Double Hydroxide for Degradation of Malachite Green. *Ecological Engineering and Environmental Technology*, 24(2), 109–119. DOI: 10.12912/27197050/157093.

[29] Wang, J., Lv, G., Wang, C. (2021). A highly efficient and robust hybrid structure of CoNiN@NiFe LDH for overall water splitting by accelerating hydrogen evolution kinetics on NiFe LDH. *Applied Surface Science*, 570, 151182. DOI: 10.1016/j.apsusc.2021.151182.

[30] Hu, X., Zhu, X., Sun, Z. (2019). Efficient flame-retardant and smoke-suppression properties of $MgAlCO_3$-LDHs on the intumescent fire retardant coating for steel structures. *Progress in Organic Coatings*, 135, 291–298. DOI: 10.1016/j.porgcoat.2019.06.014.

[31] Mohapatra, L., Parida, K.M. (2012). Zn-Cr layered double hydroxide: Visible light responsive photocatalyst for photocatalytic degradation of organic pollutants. *Separation and Purification Technology*, 91, 73–80. DOI: 10.1016/j.seppur.2011.10.028.

[32] Lesbani, A., Mohadi, R. (2014). Brönsted acid of Keggin type polyoxometalate catalyzed pinacol rearrangement. *Bulletin of Chemical Reaction Engineering and Catalysis*, 9(2), 136–141. DOI: 10.9767/bcrec.9.2.6074.136-141.

[33] Hadnadjev-Kostic, M., Vulic, T., Marinkovic-Neducin, R. (2014). Solar light induced rhodamine B degradation assisted by TiO_2-Zn-Al LDH based photocatalysts. *Advanced Powder Technology*, 25(5), 1624–1633. DOI: 10.1016/j.apt.2014.05.015.

[34] Miao, Y. fang, Guo, R. tang, Gu, J. wen, Liu, Y. zhen, Wu, G. lin, Duan, C. peng, Zhang, X. dong, Pan, W. guo (2020). Fabrication of ß-In_2S_3/NiAl-LDH heterojunction photocatalyst with enhanced separation of charge carriers for efficient CO_2 photocatalytic reduction. *Applied Surface Science*, 527, 146792. DOI: 10.1016/j.apsusc.2020.146792.

[35] Wang, J.A., Chen, L.F., Noreña, L.E. (2008). Al-MCM-41 and Pt/$H_3PW_{12}O_{40}$/Al-MCM-41: structure characterization and catalytic properties. *Studies in Surface Science and Catalysis*, 174(B), 1259–1262. DOI: 10.1016/S0167-2991(08)80117-6.

[36] Mirzaei, M., Eshtiagh-Hosseini, H., Hassanpoor, A. (2019). Different behavior of PDA as a preorganized ligand versus PCA ligand in constructing two inorganic-organic hybrid materials based on Keggin-type polyoxometalate. *Inorganica Chimica Acta*, 484, 332–337. DOI: 10.1016/j.ica.2018.09.053.

[37] Zhao, M., Fang, Y., Ma, L., Zhu, X., Jiang, L., Li, M., Han, Q. (2020). Synthesis, characterization and in vitro antibacterial mechanism study of two Keggin-type polyoxometalates. *Journal of Inorganic Biochemistry*, 210, 111131. DOI: 10.1016/j.jinorgbio.2020.111131.

[38] Astuti, Y., Elesta, P.P., Widodo, D.S., Widiyandari, H., Balgis, R. (2020). Hydrazine and urea fueled-solution combustion method for Bi_2O_3 synthesis: Characterization of physicochemical properties and photocatalytic activity. *Bulletin of Chemical Reaction Engineering & Catalysis*, 15(1), 104–111. DOI: 10.9767/bcrec.15.1.5483.104-111.

[39] Timár, Z., Varga, G., Muráth, S., Kónya, Z., Kukovecz, Á., Havasi, V., Oszkó, A., Pálinkó, I., Sipos, P. (2017). Synthesis, characterization and photocatalytic activity of crystalline Mn(II) Cr(III)-layered double hydroxide. *Catalysis Today*, 284, 195–201. DOI: 10.1016/j.cattod.2016.12.037.

[40] Ahmad, M., Ahmed, E., Ahmed, W., Elhissi, A., Hong, Z.L., Khalid, N.R. (2014). Enhancing visible light responsive photocatalytic activity by decorating Mn-doped ZnO nanoparticles on graphene. *Ceramics International*, 40, 10085–10097. DOI: 10.1016/j.ceramint.2014.03.184.

[41] Parida, K.M., Baliarsingh, N., Patra, B.S., Das, J. (2007). Copperphthalocyanine immobilized Zn/Al LDH as photocatalyst under solar radiation for decolorization of methylene blue. *Journal of Molecular Catalysis A: Chemical*, 267(1–2), 202–208. DOI: 10.1016/j.molcata.2006.11.035.

[42] Tabatabaeian, R., Dinari, M., Aliabadi, H.M. (2021). Cross-linked bionanocomposites of hydrolyzed guar gum/magnetic layered double hydroxide as an effective sorbent for methylene blue removal. *Carbohydrate Polymers*, 257, 117628. DOI: 10.1016/j.carbpol.2021.117628.

[43] Gonçalves, R.G.L., Mendes, H.M., Bastos, S.L., D'Agostino, L.C., Tronto, J., Pulcinelli, S.H., Santilli, C.V., Neto, J.L. (2020). Fenton-like degradation of methylene blue using Mg/Fe and MnMg/Fe layered double hydroxides as reusable catalysts. *Applied Clay Science*, 187, 105477. DOI: 10.1016/j.clay.2020.105477.

[44] Nayak, S., Parida, K.M. (2016). Nanostructured CeO_2/MgAl-LDH composite for visible light induced water reduction reaction. *International Journal of Hydrogen Energy*, 41(46), 21166–21180. DOI: 10.1016/j.ijhydene.2016.08.062.

[45] Li, Q., Kang, Z., Mao, B., Wang, E., Wang, C., Tian, C., Li, S. (2008). One-step polyoxometalate-assisted solvothermal synthesis of ZnO microspheres and their photoluminescence properties. *Materials Letters*, 62(16), 2531–2534. DOI: 10.1016/j.matlet.2007.12.041.